

## Chapter 22 - STANDARD PLOTS

The first tool used to understand SANS data consists of a set of **standard plots** that **yield results right after data reduction**. These are **linear plots** of functions of the scattered intensity  $I(Q)$  plotted against functions of the scattering variable  $Q$ . Note that the absolute intensity  $I(Q)$  is a short hand notation for the macroscopic scattering cross section  $d\Sigma(Q)/d\Omega$ .

### 1. THE GUINIER PLOT

The **Guinier plot** involves plotting  $\text{Ln}[I(Q)]$  vs  $Q^2$  ( $\text{Ln}$  refers to natural logarithm) in order to **obtain** the slope  $R_g^2/3$  ( $R_g$  is the radius of gyration of the scattering objects). The expansion is as follows:

$$I(Q) = I_0 \exp\left(-\frac{Q^2 R_g^2}{3}\right) \quad (1)$$
$$\text{Ln}[I(Q)] = \text{Ln}[I_0] - \frac{Q^2 R_g^2}{3}.$$

The radius of gyration represents the effective size of the scattering "particle" whether it is a polymer chain, part of a protein, a micelle, or a domain in a multiphase system. The usefulness of this plot stems from the fact that the obtained particle "size"  $R_g$  is independent of the absolute intensity  $I_0$  and of any model. Instrumental smearing as well as polydispersity and multiple scattering appear to decrease the effective  $R_g$ . Inter-particle effects also contribute to  $R_g$  except at the infinite dilution limit (case of an isolated particle).

Consider the Guinier plot for a solution of Pluronic P85 in  $D_2O$ . Pluronic are triblock copolymers of poly(ethylene oxide)-poly(propylene oxide)-poly(ethylene oxide), i.e., PEO-PPO-PEO. At low temperature, both PEO and PPO dissolve in water so that SANS observes isolated polymer chains. This is the case for 20 °C. The radius of gyration obtained from the Guinier plot gives an estimate of polymer chain dimension. A Guinier plot is shown for 10 % (g/g) P85 in  $D_2O$  measured at 20 °C.

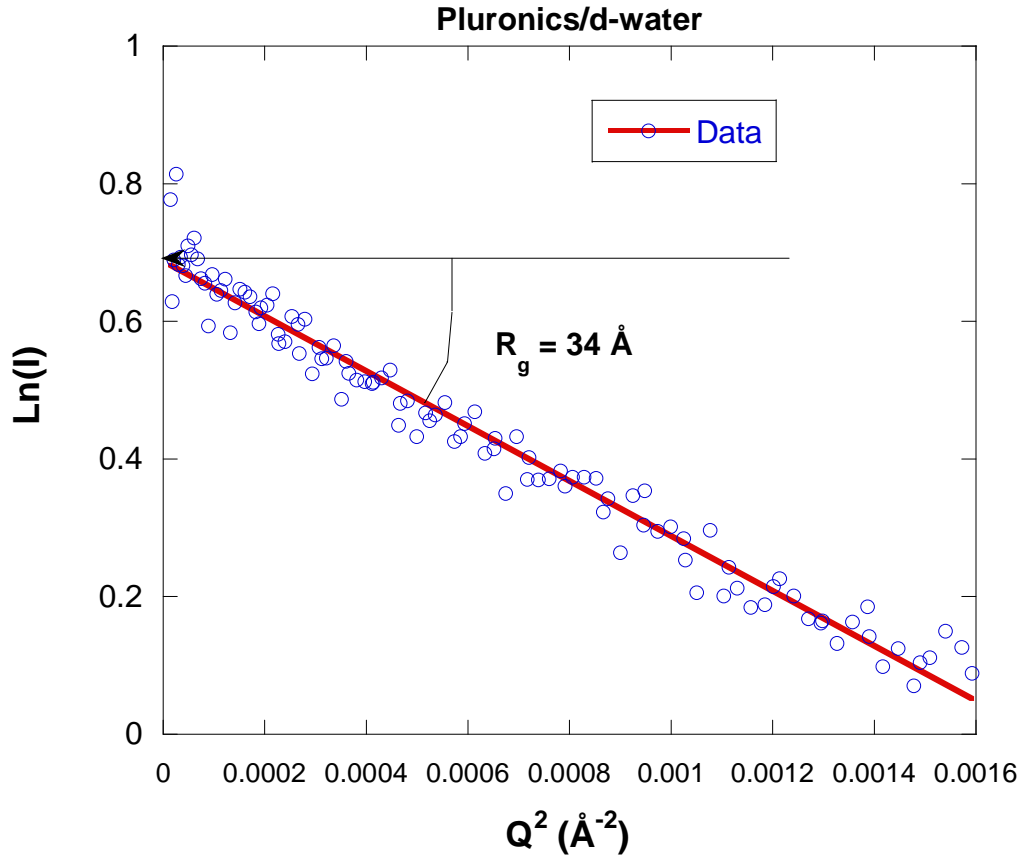


Figure 1: **Guinier plot** for SANS data taken from **10 % (g/g) P85 Pluronic in D<sub>2</sub>O at 20 °C**. The slope of the Guinier plot is  $R_g^2/3$ .

Note that at higher temperatures, PPO does not dissolve in water so that P85 forms micelles with PPO forming the core and PEO forming an outside shell. An inter-particle peak forms and the Guinier plot can no longer be used. Other methods used to analyze such SANS data will be described later.

Another example of a Guinier plot is for SANS data from a solution of PAMAM dendrimers formed of seven generations and dissolved in D<sub>2</sub>O. The dendrimer fraction (g/g) is varied in the dilute solution range. No acid or salt has been added. The apparent radius of gyration is seen to decrease with dendrimer fraction.

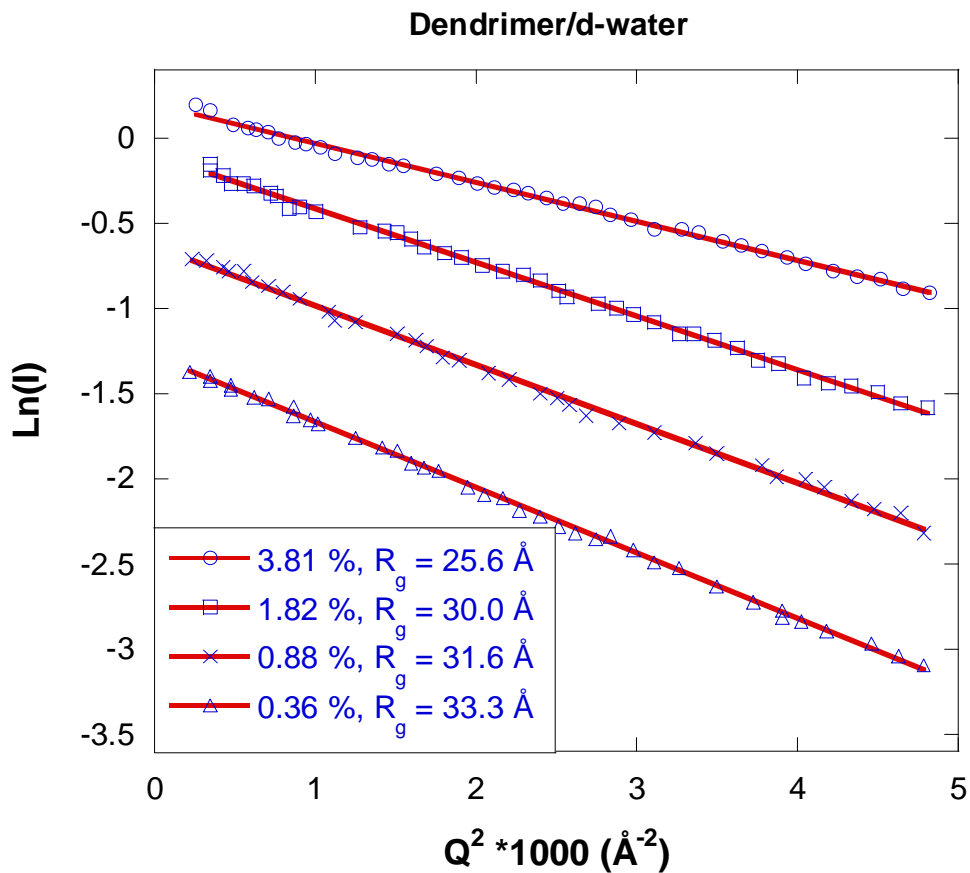


Figure 2: **Guinier plot** for SANS data taken from seventh-generation **PAMAM dendrimers** in  $D_2O$ . The dendrimer fraction is varied.

The range of a **Guinier plot** corresponds to  $QR_g < \sqrt{3}$ . This is obtained when the probed range ( $2\pi/Q$ ) is larger than the particle size.

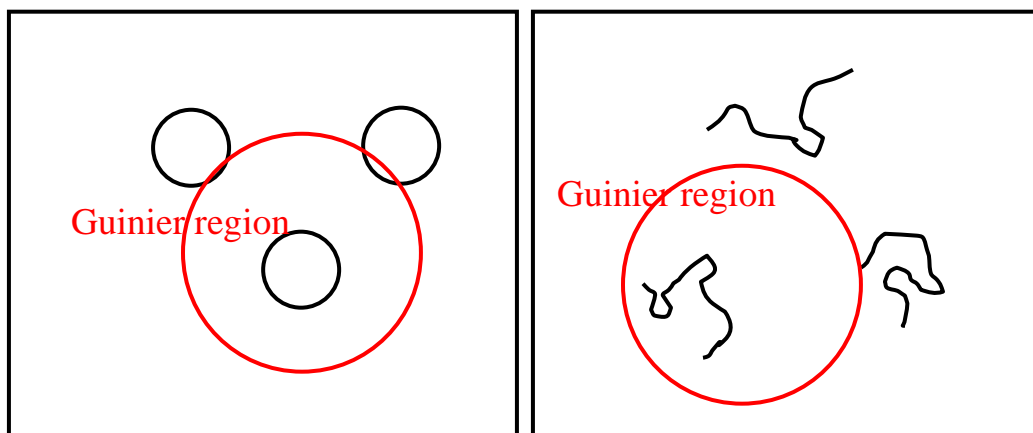


Figure 3: Scattering particles are smaller than the probed range in the Guinier region shown for isolated particles and for single polymer coils.

## 2. THE GUINIER PLOT FOR ELONGATED OBJECTS

The Guinier plot is modified when the scattering objects are elongated (Glatter-Kratky, 1982). For instance, for a cylinder of length  $L$  and radius  $R$ , the low- $Q$  Guinier approximation remains:

$$I(Q) = I(0) \exp\left(-\frac{Q^2 R_g^2}{3}\right) \quad \text{where } R_g^2 = \frac{L^2}{12} + \frac{R^2}{2}. \quad (2)$$

The low- $Q$  Guinier plot is still  $\text{Ln}[I(Q)]$  vs  $Q^2$ . The intermediate- $Q$  Guinier approximation is different:

$$I(Q) = \frac{I(0)}{Q} \exp\left(-\frac{Q^2 R_g^2}{2}\right) \quad \text{where } R_g^2 = \frac{R^2}{2}. \quad (3)$$

The intermediate- $Q$  Guinier plot becomes  $\text{Ln}[QI(Q)]$  vs  $Q^2$ . A figure shows the form factor for a cylinder of length  $L = 345 \text{ \AA}$  ( $R_{g2} = \sqrt{L^2/12 + R^2/2} = 100 \text{ \AA}$ ) and radius  $R = 14 \text{ \AA}$  ( $R_{g1} = \sqrt{R^2/2} = 10 \text{ \AA}$ ).

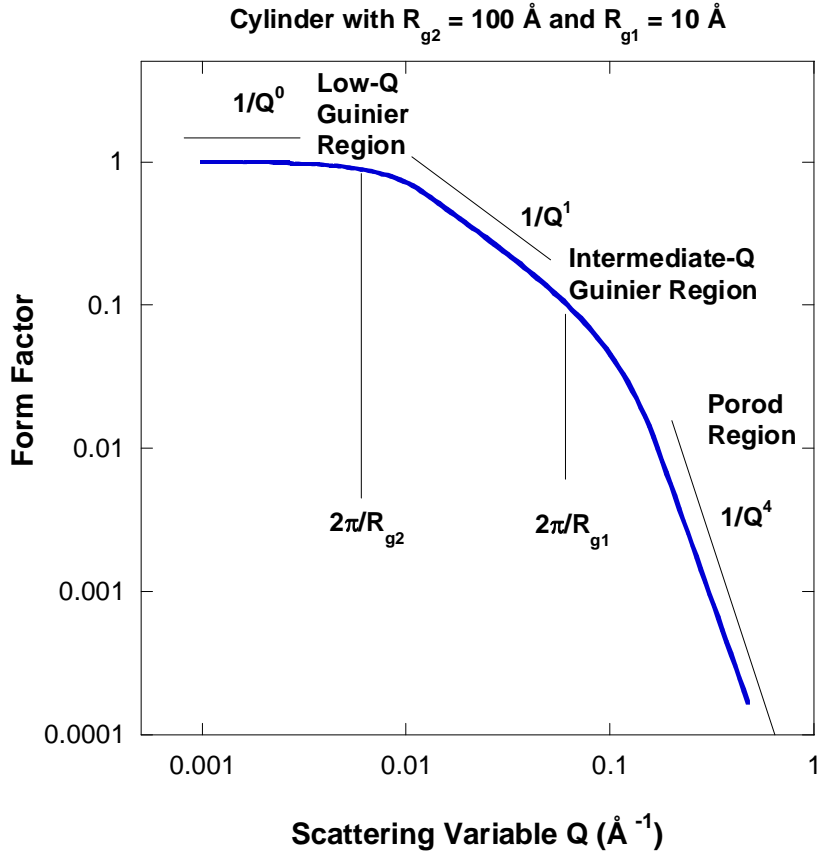


Figure 4: Form factor for a cylinder showing the low-Q Guinier region, the intermediate-Q Guinier region and the high-Q Porod region.

Similarly for a lamella (flat object) of thickness  $T$ , the intermediate-Q Guinier approximation becomes:

$$I(Q) = \frac{I(0)}{Q^2} \exp\left(-\frac{Q^2 R_g^2}{1}\right) \quad \text{where } R_g^2 = \frac{T^2}{12}. \quad (4)$$

The intermediate-Q Guinier plot becomes  $\text{Ln}[Q^2 I(Q)]$  vs  $Q^2$ .

### 3. THE POROD LAW

Consider the case of an infinitely dilute solution of spheres of radius  $R$  and smooth surfaces. The scattering intensity is given by:

$$I(Q) = \left(\frac{N}{V}\right) \Delta\rho^2 V_p^2 F^2(QR). \quad (5)$$

The standard characteristic parameters have been defined as:  $(N/V)$  is the spheres number density,  $\Delta\rho^2$  is the contrast factor,  $V_p$  is the sphere volume and  $F(QR)$  is the single-sphere form factor amplitude given as follows:

$$F(QR) = \frac{3j_1(QR)}{QR} = \frac{3}{QR} \left( \frac{\sin(QR)}{(QR)^2} - \frac{\cos(QR)}{QR} \right). \quad (6)$$

Note that the single-sphere form factor  $P(QR) = F^2(QR)$  is also defined as:

$$P(QR) = \int d^3r \exp[-i\vec{Q}\cdot\vec{r}] P(\vec{r}) = \frac{1}{V_p} \int_0^\infty dr 4\pi r^2 \frac{\sin(Qr)}{Qr} \gamma(r). \quad (7)$$

Here the pair correlation function  $P(\vec{r})$  has been defined. The pair correlation function  $P(\vec{r})$  is the probability of finding a scatterer at a vector distance  $\vec{r}$  inside the sphere knowing that there is another scatterer at the origin.  $\gamma(r)$  is the equivalent 1D probability distribution defined radially. Consider a sphere of radius  $R$  and a scatterer located at a radial distance  $r'$  from the sphere origin. Draw another sphere of radius  $r$ .  $\gamma(r)$  represents the relative fraction of area of the second sphere located inside the large sphere integrated over all possible locations. Defining that relative fraction as  $p(r,r')$ , the following two cases can be considered:

$$\begin{aligned} p(r,r') &= 1 & R-r > r' & \quad (8) \\ p(r,r') &= \frac{1}{2} + \frac{1}{4} \left[ \frac{R^2 - r^2 - r'^2}{rr'} \right] & R-r \leq r'. & \end{aligned}$$

The radial pair correlation function for a sphere is therefore (Stein et al, 1963):

$$\gamma(r) = \frac{\int_0^{R_A} dr' 4\pi r'^2 p(r,r')}{\int_0^{R_A} dr' 4\pi r'^2} = 1 - \frac{3}{4} \left( \frac{r}{R} \right) + \frac{1}{16} \left( \frac{r}{R} \right)^3. \quad (9)$$

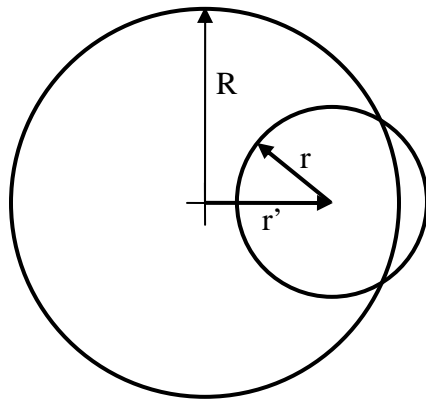


Figure 4: Representation of the geometry used to calculate the radial pair correlation function for a sphere.

The pair correlation function  $\gamma(r)$  is the 3D Fourier transform of the single particle scattering factor  $P(Q)$ . The 1D sine Fourier transform of  $P(Q)$  is  $r\gamma(r)$ .

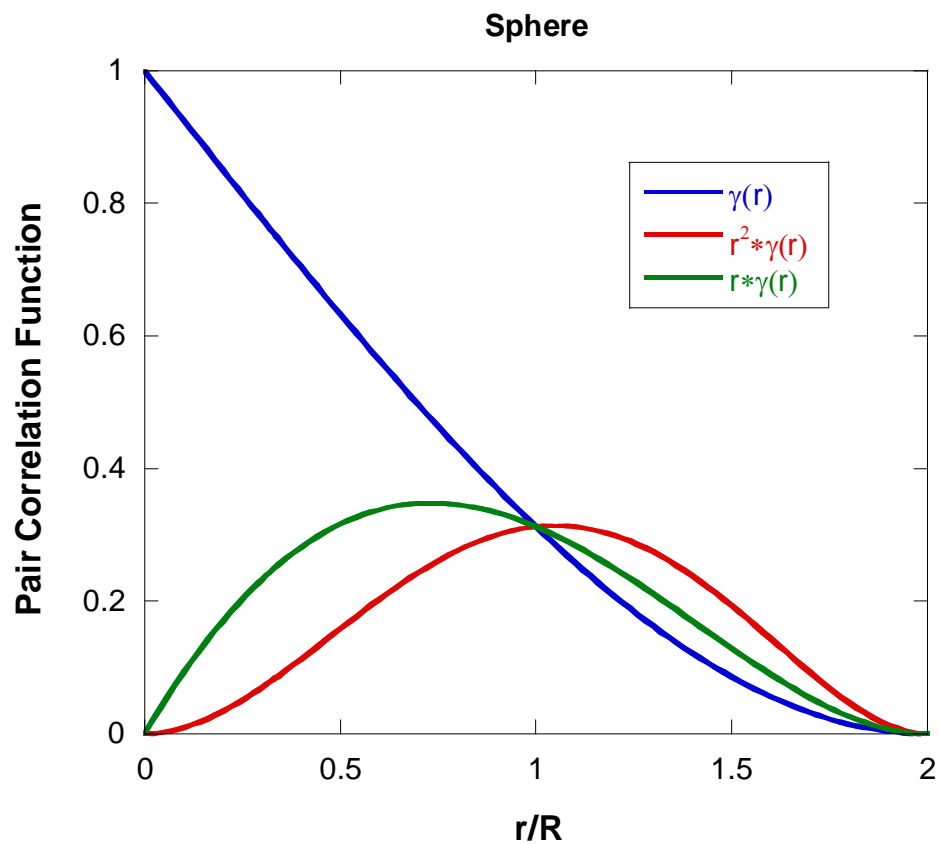


Figure 5: Plot of the pair correlation function  $\gamma(r)$ , of  $r^2\gamma(r)$  and of  $r\gamma(r)$ .

Using this form,  $P(QR)$  can be expressed as follows:

$$P(QR) = \frac{1}{V_P} \int_0^\infty dr 4\pi r^2 \frac{\sin(Qr)}{Qr} \left[ 1 - \frac{3}{4} \left( \frac{r}{R} \right) + \frac{1}{16} \left( \frac{r}{R} \right)^3 \right]. \quad (10)$$

Note that this is the well known form factor for a sphere  $P(QR) = [3j_1(QR)/QR]^2$  introduced earlier. The interest here is in the high-Q expansion. The highest order in this expansion is obtained by integrating by parts three times:

$$P(QR) \sim -\frac{4\pi}{V_P} \frac{2\gamma'(0)}{Q^4} = \frac{S_P}{V_P R^2} \frac{3}{2Q^4 R} = \frac{3}{2R^3} \left( \frac{S_P}{V_P} \right) \frac{1}{Q^4}. \quad (11)$$

$(S_P/V_P)$  is the surface to volume ratio. This is the so-called Porod law.

The scattering intensity can simply be expressed as  $I(Q) = A/Q^4 + B$  where B is the constant (mostly incoherent) scattering background.

#### 4. THE POROD PLOT

The Porod region corresponds to a probed range smaller than the scattering objects so that the scattering radiation is probing the local structure. The Porod plot  $\text{Log}(I)$  vs  $\text{Log}(Q)$  (Log is base-10 logarithm) yields information about the so-called "fractal dimension" of the scattering objects. At high-Q, one can approximate:

$$I(Q) = \frac{A}{Q^n} + B \quad \text{or} \quad \text{Log}[I(Q) - B] = \text{Log}(A) - n\text{Log}(Q). \quad (12)$$

A Porod slope  $n = 1$  is obtained for scattering from rigid rods; a slope  $n = 4$  represents a smooth surface for the scattering particle; whereas a slope  $n$  between 3 and 4 characterizes rough interfaces of fractal dimension D with  $n = 6-D$ . This is called a surface fractal.

Moreover, in the case of polymer coils, the Porod slope  $n$  is related to the excluded volume parameter  $v$  as its inverse  $n = 1/v$ . A slope  $n = 2$  is a signature of Gaussian chains in a dilute environment, a slope  $n = 5/3$  is for fully swollen coils and a slope  $n = 3$  is for collapsed polymer coils. A slope between 2 and 3 is for "mass fractals" such as branched systems (gels) or networks.

An example of a Porod plot is shown for SANS data from a 4 % (g/g) solution of salmon DNA in d-ethylene glycol) at a temperature of 50 °C. At this temperature, the helical structure has melted into coil conformation. 1 M NaCl salt has been added in order to screen charge interactions. The slope of the Porod plot of  $n = 1.76$  is close to the value  $n = 5/3 = 1.667$  which is a signature for fully swollen coils.



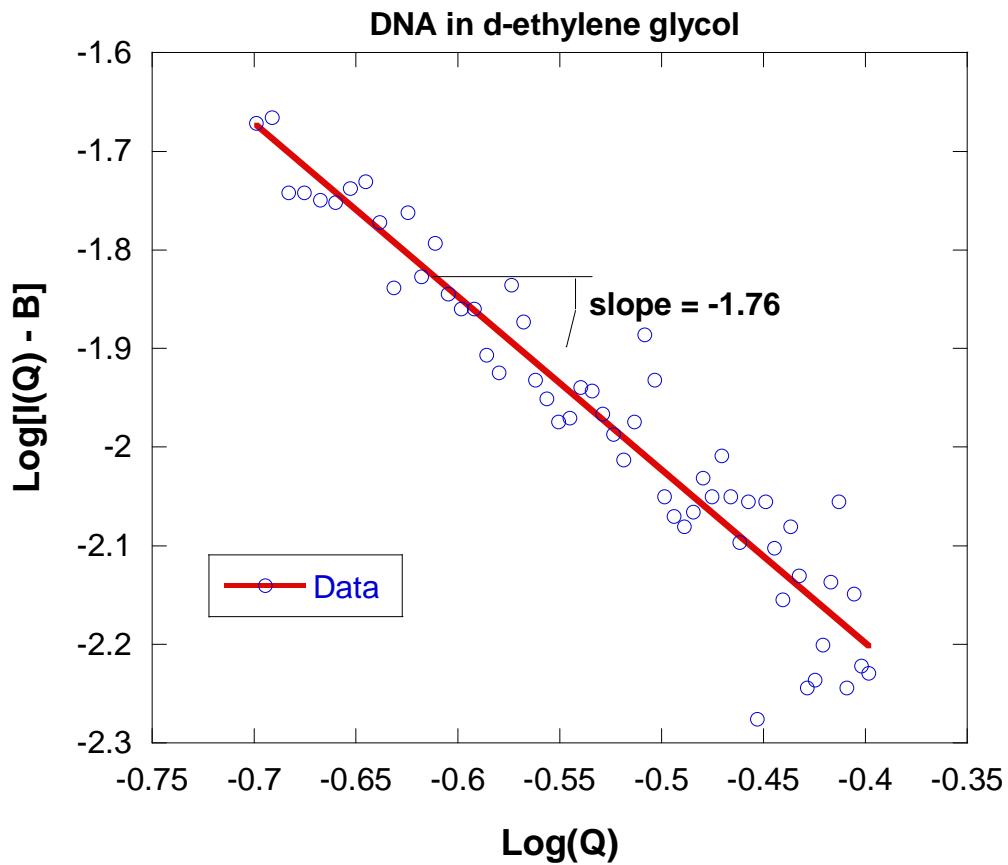


Figure 6: **Porod plot** for SANS data taken from 4 % (g/g) DNA coils in d-ethylene glycol at 50 °C (above the helix-to-coil transition temperature). 0.1 M NaCl was added to screen charge interactions.

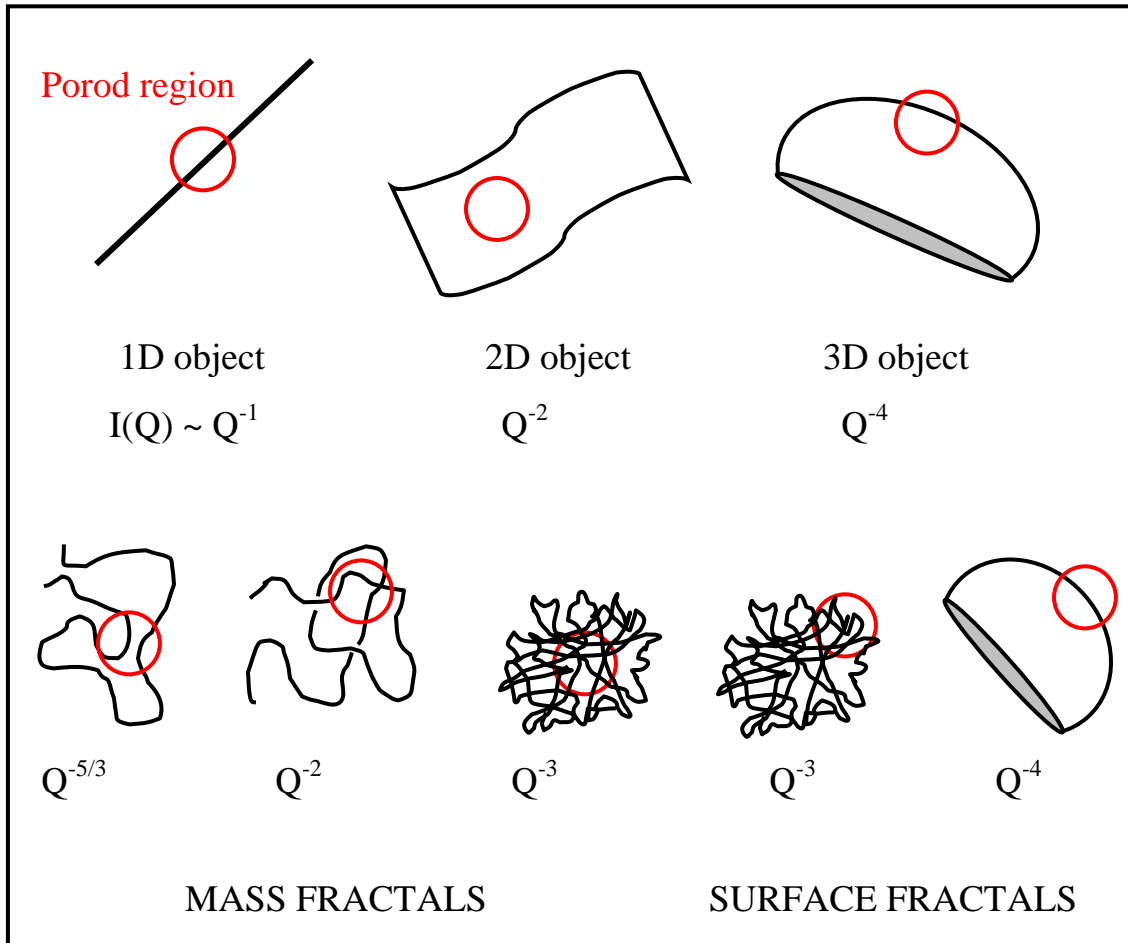


Figure 7: Assortment of Porod law behaviors for different shape objects.

## 5. THE ZIMM PLOT

Another well known plot is the Zimm plot ( $1/I$  vs  $Q^2$ ) which found wide use in light scattering from dilute polymer solutions where extrapolation to zero  $Q$  and zero concentration yields the molecular weight, the radius of gyration and the second virial coefficient. The Zimm plot is also useful in polymer blends (in the single-phase region) where the slope is proportional to the correlation length, which is proportional to the Flory-Huggins interaction parameter (incompressible RPA model) to be described later.

Assume a Lorentzian form for the  $Q$ -dependence of the scattering intensity:

$$I(Q) = \frac{I_0}{1 + Q^2 \xi^2}. \quad (13)$$

Here  $\xi$  is the correlation length. A plot of  $1/I(Q)$  vs  $Q^2$  yields  $1/I_0$  as intercept and  $\xi^2/I_0$  as slope. The correlation length is obtained as  $\xi = (\text{slope/intercept})^{1/2}$ . In the low-Q region, one can also expand:

$$I(Q) = \frac{I_0}{1 + \frac{Q^2 R_g^2}{3}} = I_0 \left( 1 - \frac{Q^2 R_g^2}{3} + \dots \right). \quad (14)$$

Therefore yielding  $\xi = R_g / \sqrt{3}$  for low-Q. The Zimm plot applies, however, beyond the low-Q region. In the high-Q region where  $Q^2 \xi^2 < 1$ , one can approximate:

$$\frac{1}{I(Q)} = \frac{Q^2 \xi^2}{I_0}. \quad (15)$$

In this region, the single polymer chain form factor behaves as  $2/Q^2 R_g^2$  (high-Q expansion of the Debye function) so that  $\xi = R_g / \sqrt{2}$  is identified for high-Q. In the case of polymer solutions with excluded volume interactions, the high-Q expansion is, instead:

$$I(Q) = I_0 \frac{2}{(QR_g)^{1/\nu}}. \quad (16)$$

Here  $\nu$  is the excluded volume exponent ( $\nu = 3/5$  for fully swollen chains,  $\nu = 1/2$  for theta chains and  $\nu = 1/3$  for collapsed chains).

Low-Q departure from linear behavior of the Zimm plot is a signature of non-homogeneity in the sample or of chain-branching. A negative value of the intercept  $I_0$  (obtained through extrapolation) is a sign of phase separation.

An example of a Zimm plot is shown for SANS data taken from a blend mixture of poly(ethyl butylene) and deuterated poly(methyl butylene); i.e., hPEB/dPMB. The molecular weights for hPEB/dPMB are  $M_w = 40,100$  g/mol and  $88,400$  g/mol respectively. The volume fraction of the represented sample corresponds to 57 % hPEB. This blend mixture was measured at a temperature of 10 °C. The Zimm plot is linear pointing to Gaussian chains. The slope yields an apparent radius of gyration which depends on the polymer/polymer interaction parameter. These issues will be described in detail when the Random Phase Approximation (RPA) model is introduced.

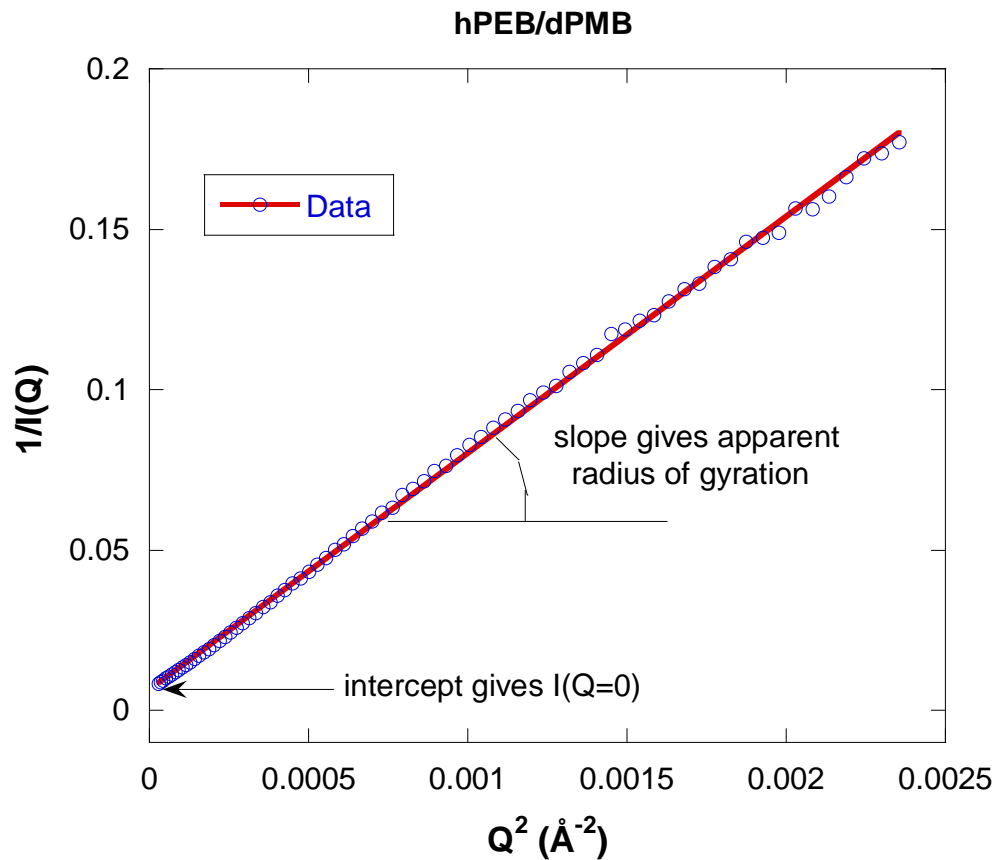


Figure 8: Zimm plot for a polymer blend mixture of hPEB and dPMB with  $M_w = 40,100$  g/mol, and 88,400 g/mol respectively. The hPEB fraction is 57 % (g/g) and the measurement temperature is 10 °C (single-phase region).

A more detailed Zimm plot is for SANS data from a polymer blend mixture of deuterated polystyrene and poly(vinyl methyl ether); i.e., dPS/PVME (Briber et al, 1994). Four dilute dPS volume fractions were measured at a temperature of 140 °C. The dPS/PVME blend system is characterized by a Lower Critical Spinodal temperature (LCST) and 140 °C corresponds to the single-phase region. Extrapolation to zero volume fraction yields a slope and intercept which give the degree of polymerization for polystyrene and the radius of gyration respectively.

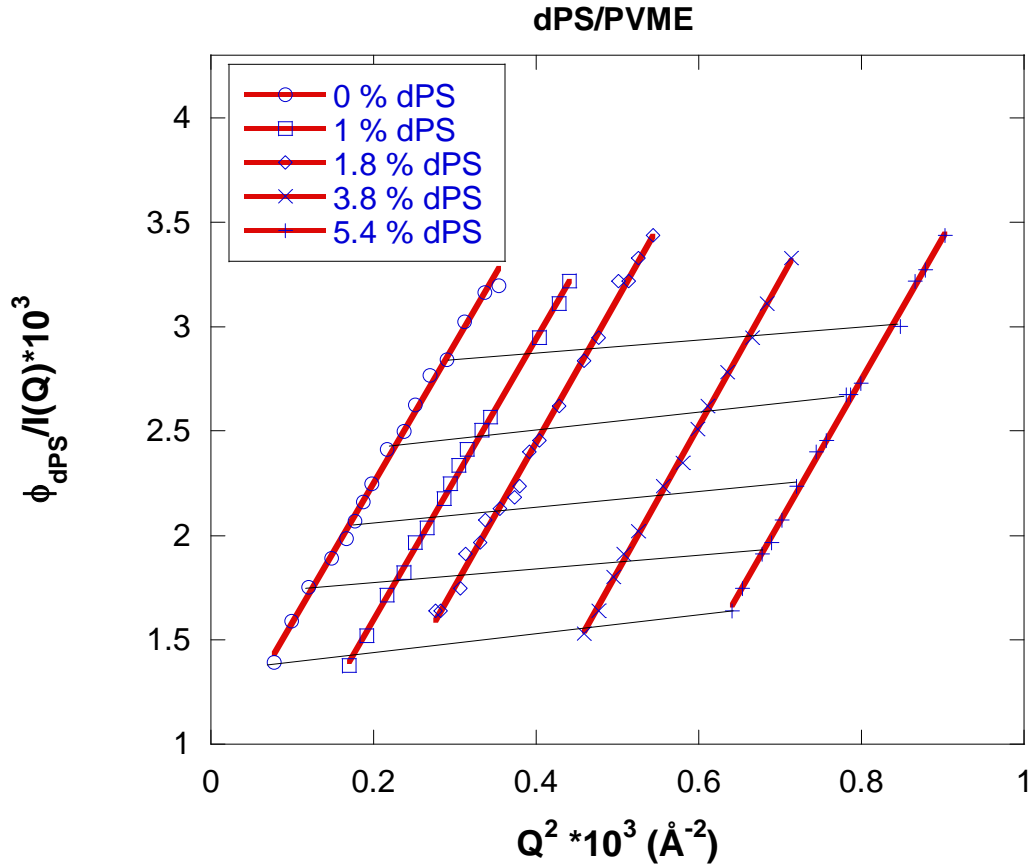


Figure 9: Zimm plot for a deuterated polystyrene/polyvinylmethylether blend ( $M_w = 1.88 \cdot 10^5$  g/mol and  $3.98 \cdot 10^5$  g/mol respectively) mixture for four dilute polystyrene volume fractions of  $\phi_{dPS} = 1\%$ ,  $1.8\%$ ,  $3.8\%$  and  $5.4\%$  at a temperature of  $140^\circ\text{C}$ .

## 6. THE KRATKY PLOT

Kratky plots emphasize deviation from the high-Q behavior of the scattering intensity  $I(Q)$ . For polymer chains, the Kratky plot ( $Q^2 I(Q)$  vs  $Q$ ) emphasizes the Gaussian chain nature or departure from it. Since the form factor for Gaussian chains varies like  $I(Q) \sim 1/Q^2$  at high-Q, this plot tends to a horizontal asymptote. Inter-chain contributions affect only the constant multiplying this term and not the  $1/Q^2$  scaling behavior. Deviation from a horizontal asymptotic behavior indicates a non-Gaussian characteristic for the scattering chains.

For instance, for rigid rods this plot would go to a linearly increasing asymptote  $Q^2 I = A + BQ$  because the form factor for a rod varies like  $I(Q) \sim 1/Q$  at high  $Q$  and one has to use a more suitable Kratky plot for a rod ( $QI$  vs  $Q$ ) in order to recover the horizontal asymptote. In order to illustrate this in simple terms, three functions that die out differently at high  $Q$  are considered. These three cases are (1) for rigid rods where  $I(x) =$

$I_0/(1+x)$ , (2) for Gaussian chains where  $I(x) = I_0/(1+x^2)$ , and (3) for branched systems (or mass fractals) where  $I(x) = I_0/(1+x^3)$ . Here  $x$  is the dimensionless variable  $x = Q\xi$  where  $\xi$  is a characteristic length (radius of gyration or correlation length). These functions reproduce the proper low  $x$  and high  $x$  limits.

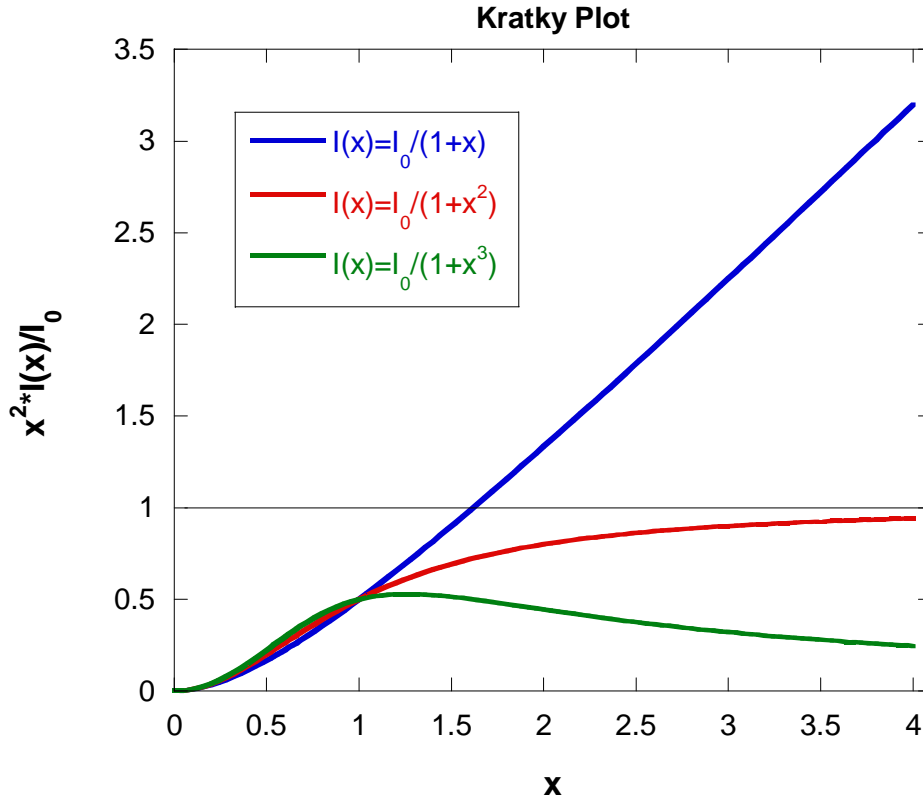


Figure 10: Symbolic representation of the **Kratky plot** for the three cases of a **rigid rod**, a **Gaussian chain** and a **mass fractal**.

Gaussian chains tend to the Kratky plot limit of 1. Stiff chains (for example rigid rods) increase linearly at high  $x$  and branched systems (mass fractals) reach a maximum then decrease as  $1/x$  at high  $x$ .

An example of a Kratky plot is shown for SANS data taken from an isotopic blend mixture of deuterated polystyrene with non-deuterated polystyrene, i.e., dPS/hPS with  $M_w = 174,000$  g/mol and  $195,000$  g/mol respectively at 50 % fraction (g/g) and measured at ambient temperature. This plot represents the Gaussian nature of polymer chains in isotopic blends and tends to the asymptote of 1 at high  $Q$ .

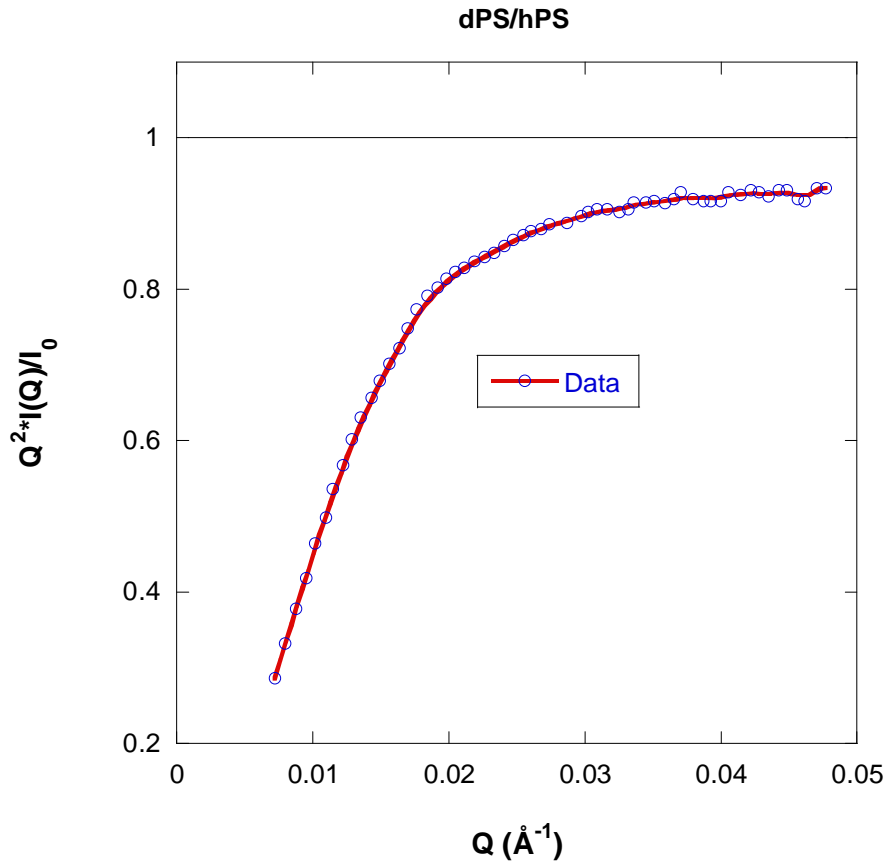


Figure 11: **Kratky plot** for an **isotopic blend mixture** of dPS and hPS with  $M_w = 174,000$  g/mol and  $195,000$  g/mol, 50 % fraction (g/g) measured at ambient temperature. The line is a smoothing fit as a guide to the eye.

Another Kratky plot is shown for a seventh generation PAMAM dendrimer in  $D_2O$ . SANS data were taken from a series of dilute solutions and extrapolated to the infinite dilution limit (Hammouda, 1992). Measurements were taken at ambient temperature. This plot represents the branched character of this scattering system. It has not been rescaled at high  $Q$ .

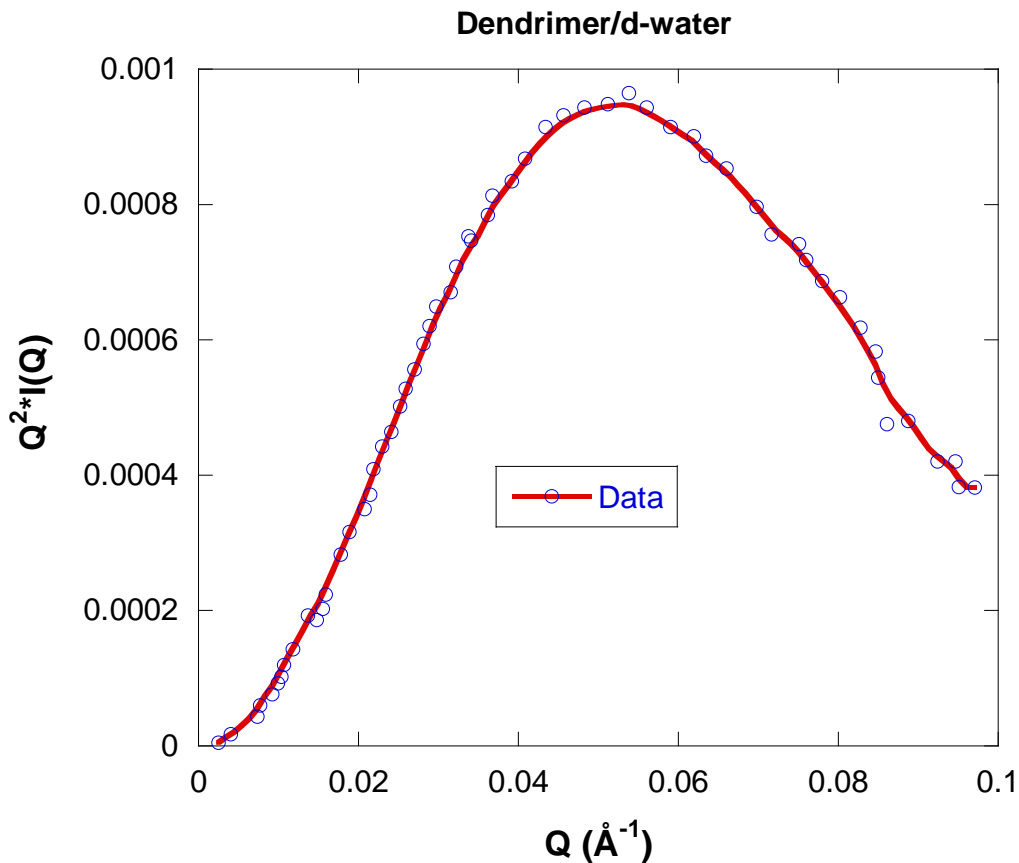


Figure 12: **Kratky plot** for seventh generation **PAMAM dendrimer solution** in  $D_2O$  extrapolated to the infinite dilution limit (zero concentration). The Katky plot reaches a maximum then tends to a constant level at high  $Q$ .

The manner in which the asymptote of a Kratky plot is reached yields information about chain branching. For instance, in a plot of  $Q^2 I$  vs  $1/Q^2$  ( $Q^2 I = A + B/Q^2$ ) the intercept  $B$  is related to the crosslink density in branched gels and networks (Benoit et al, 1993).

## REFERENCES

O. Glatter, and O. Kratky, "Small-Angle X-Ray Scattering", Academic Press (1982).

R.S. Stein, P.R. Wilson and S.N. Stidham, "Scattering of Light by Heterogeneous Spheres", *J. Applied Physics* **34**, 46-50 (1963)

B. Hammouda, "Structure Factor for Starburst Dendrimers", *J. Polym. Sci., Polym. Phys. Ed.*, **30**, 1387-1390 (1992)

R.M. Briber, B.J. Bauer and B. Hammouda, "SANS from Polymer Blends in the Dilute Concentration Limit", *J. Chem. Phys.* **101**, 2592-2599 (1994)



## QUESTIONS

1. What is a Guinier Plot? What can be obtained from it? What can be obtained from the intercept?
2. Do scattering inhomogeneities have to be spherical for a radius of gyration to be defined and measured through a Guinier plot?
3. What information could be obtained using a Porod plot for smooth interfaces?
4. How does polydispersity and instrumental smearing affect the Guinier plot and the Porod plot?
5. Consider the pair correlation function for a sphere of radius  $R_A$ , given by:  
$$\gamma(r) = 1 - \frac{3}{4} \left( \frac{r}{R} \right) + \frac{1}{16} \left( \frac{r}{R_A} \right)^3$$
. Explain the limit  $g(r=2R_A) = 0$ .
6. A Zimm plot is linear for what scattering objects?
7. What information can be obtained from a Kratky plot?

## ANSWERS

1. A Guinier plot is a plot of  $\ln(I)$  vs  $Q^2$ . The radius of gyration ( $R_g$ ) can be obtained from the slope of a Guinier plot (slope =  $R_g^2/3$ ). The intercept of a Guinier plot is  $I(0)$  which can yield the aggregation number which is the number of basic scattering units per scattering "particle". A scattering unit could be a monomer and a scattering particle could be a polymer.
2. The Guinier plot  $\ln(I)$  vs  $Q^2$  measures a radius of gyration from any shape objects. These do not have to be globular.
3. The Porod plot  $\log(I)$  vs  $\log(Q)$  for scattering objects with smooth interfaces yields an exponent from the slope and a surface-to-volume ratio from the intercept.
4. Polydispersity and instrumental smearing yield broader forward scattering peaks and therefore a lower radius of gyration from the Guinier plot. These, however, do not affect the Porod exponent which remains unchanged.
5. Consider a scatterer inside a sphere of radius  $R_A$  and draw another sphere of radius  $r$ . Choosing the first scatterer on the surface of the sphere and choosing a second sphere of radius  $r = R_A$  covers the maximum correlation range of  $2R_A$ . Beyond that range, scatterers are not correlated.
6. A Zimm plot  $1/I$  vs  $Q^2$  is linear for Gaussian polymer coils.
7. A Kratky plot  $\log(Q^2I)$  vs  $Q$  saturates to a constant level at high- $Q$  for flexible polymer coils but increase linearly for rigid rods. The break between the constant and the linear behaviors yields an estimate of the so-called persistence length which is a measure of chain stiffness.